Mine Water and the Environment (2022) 41:979–995
https://doi.org/10.1007/s10230-022-00890-7

TECHNICAL ARTICLE

Investigation of a Method to Prevent Rock Failure and Disaster Due to a Collapse Column Below the Mine

Bo Ren[1,2] · Liang Yuan[1,2,4] · Wenqiang Mu[3] · Yongshu Zhang[3] · Guofeng Yu[1,4] · Chengping Cao[1] · Minhua Wang[5] · Yong Luo[1] · Lianchong Li[3]

Received: 21 May 2021 / Accepted: 13 July 2022 / Published online: 29 August 2022

Abstract

With increased mining depth, water inrush accidents have become one of the main mine disasters in China. A three-dimensional prevention and control method (3DPCM) consisting of first probe drilling from the ground surface, then grouting, and then real-time measurement was proposed. The method was applied to solve the potential risk in a mine with a coal floor underlain by a pressurized aquifer. The numerical calculations, the effect of grouting in the collapse zone, and the stress distribution are discussed. The research shows that combining downhole and cross hole seismic with borehole exploration can identify and characterize important structures. Based on the geological and hydraulic characteristics, multi-layer high-pressure grouting was used to reduce the water inflow to about zero. Then, based on microseismic (MS) technology, real-time monitoring was carried out to evaluate the performance of the grouted rock as mining progressed. The grouted area showed the expected improvement of mechanical properties with no observed failure. The MS survey showed significant improvement and reduced deformation in the grouted zone to a radius of about 60 m. The collapse zone showed a long-term stress concentration factor of 1.2, which further shows that grouting can change the stress distribution in the mining area. 3DPCM can achieve comprehensive mitigation and control of abnormal geological structures. This study can help solve the problem of deep mine water inrushes and associated disasters.

Keywords Water inrush · Mine floor · Collapse column · Microseismic monitoring · Numerical calculation

Introduction

The hydrogeological conditions at coal mines in China are complex, and floor water inrush has always been one of the main risks threatening the safety of coal mining (Dong et al. 2021; Hu and Zhao 2021; Li et al. 2013a, b; Wu et al. 2019; Zhang 2005; Zhang et al. 2017). In recent years, with the depletion of shallow resources and gradual increase of mining depth, the threat of a mine water inrush disaster, due to confined aquifers below the mine floor, is becoming more serious (Li et al. 2013a, b; Sun et al. 2019; Wu et al. 2017). The threat in north China coalfields is particularly serious where pressurized water in the Ordovician limestone underlies the mine excavation, beneath thin layers of aquitards. Karstic voids in the Ordovician limestone aquifer are well developed, with water under high pressure and capable of high water yield. The karstic strata have experienced multi-stage tectonic movements, which intensifies the hydraulic connection between the aquifers. As a result, the mine water inflow potential is large, and the frequency of water inrush

✉ Liang Yuan
yuanl_1960@sina.com

✉ Wenqiang Mu
neumwq2017@163.com

1 State Key Laboratory of Deep Coal Mining and Environment Protection, Coal Mining National Engineering Technology Research Institute, Huainan 232000, China

2 School of Emergency Management and Safety Engineering, China University of Mining and Technology (Beijing), Beijing 100083, China

3 School of Resources and Civil Engineering, Northeastern University, Shenyang 110819, China

4 School of Safety Science and Engineering, Anhui University of Science and Technology, Huainan 232001, China

5 Coal Industry Branch of Huaihe Energy Group, Huainan 232000, China

disasters is high (Li et al. 2021a, b; Niu et al. 2020; Song et al. 2021). The failure characteristics of the coal seam floor above the confined aquifer becomes the key to controlling the water inrush mechanism (Ma et al. 2021). Based on theoretical calculations, numerical simulations, and site monitoring, the failure mechanisms of the coal floor can be comprehensively analyzed, to provide understanding of the risk and mitigation strategies related to floor water inrush (Meng et al. 2019).

Wu et al. (2014) combined fractal and Ergun high-speed flow theory with dynamic system instability to reveal the factors influencing floor water inrush. Water inrush was found to be related to the coupled effect of the mine influenced stress regime on the rock and water pressure (Zhang 2021). Lu et al. (2015) proposed a damage and flow coupling simulation method based on micromechanics to simulate the evolution of stress-damage-seepage coupling on the progressive development of fractures in floor rock during mining above a confined aquifer. Ma et al. (2020) used the computational fluid dynamics (CFD) method to quantitatively analyze the flow of fissure water and sediment and discussed the mechanism of floor water and sediment inrush in coal mining.

Based on structural mechanics and damage mechanics, Duan et al. (2021) established a mechanical model of an idealized broken floor rock stratum. Duan et al. studied and determined the critical equations and main factors contributing to floor water inrush. Using finite element methods, Yang et al. (2021) developed a source program to simulate floor water inrush through the fracture zone. The analysis revealed the distribution and variation in the water inrush pressure field, velocity field, porosity and concentration, and provided further insight into the mechanism of water inrush. Floor water inrush was found to be significantly related to geological structure, water pressure, and mining activity. Song and Liang (2021) used a mechanical model to analyze both the failure depth in unfaulted rock, and the theoretical mechanism of maximum failure depth in faulted rock. Most of the coal mine water inrush hazard is, unsurprisingly, related to discontinuities. It was further noted that mining of a coal seam may lead to the development of new fractures related to geological structure, and fracture development shows a time lag closely related to the permeability of the discontinuities (Yu et al. 2021).

Experience shows that water inrush often occurs through a feature known as a "collapse column," which takes the shape of an elliptical cylinder (Cheng et al. 2021a, b, c; Xu et al. 2021) and (Chuai et al. 2017). Inrush can be initiated through the side wall or top–bottom of the collapse column when mining approaches the side wall or the floor/roof rock at a point where the collapse column cannot resist the water pressure. As the collapse column develops, the stress–strain distribution becomes uneven. Fractures caused or reactivated by mining activities lead to changes in hydraulic conductivity, and seepage pressure changes cause strain in the collapse column rock and surrounding strata. Seepage water can also soften the rock. Once the pressure of the confined water is greater than the minimum principal stress, hydraulic fracturing will occur and water inrush channels can be formed that connect to the mining void, resulting in an inrush disaster (Li et al. 2021a, b; Wang et al. 2009, 2010) and (Zhang et al. 2021; Zhao et al. 2020a, b). Control of a column collapse and water inrush can be achieved by detailed exploration of geological structure and effective control technology, as described in this paper.

Effective control of rock fractures in a collapse column is the key to preventing water inrush. The main factors are the ground pressure, mining scale, geological structures, and water pressure of the underlying aquifer. The aquifer and structural geological body can be transformed (reinforced) by grouting, which can block water pressure in the aquifer and increase the strength of the rock mass and discontinuities. Grouting is an effective control method often used as to control geological and hydrotechnical risks, such as floods, dam seepage (Salimiana et al. 2017; Zhang 2021), and tunnel reinforcement (Mu et al. 2019, 2021; Stromsvik 2019). Grouting has been widely used in the prevention and control of floor water seepage and inrush (Ren et al. 2021; Yuan et al. 2020). In deep large-scale coal mining operations, grouting on a regional and local discontinuity scale has become a key way to mitigate water inrush from confined aquifers.

Even in grouted ground, an inrush can be caused by secondary fracturing induced by mining. Understanding secondary disturbance fracture evolution processes and identifying precursor responses in grouted ground is key to controlling an inrush. Modern technology makes it possible to monitor the ground response (Wu et al. 2021). Hu et al. (2021) buried a network of distributed optical fiber sensors in the coal floor and obtained an almost real time estimate of the condition of the floor rock and an estimate of the failure depth using multiple regression analysis. Using microseismic (MS) data, Zhao et al. (2020a, b) identified seepage channels within the rock mass. Jin et al. (2011, 2021) established an early warning index including stress, water temperature, and water pressure, and developed a monitoring and trigger system for the coal floor water inrush hazard based on the Fiber Bragg grating system. Using MS monitoring technology, Cheng et al. (2021a, b, c) identified the spatial location and formation process of rock fractures, which allowed them to monitor the sequential development of water channels indicating precursor conditions moving towards water inrush. These monitoring systems provide a way to identify a potential water in rush problem and apply pre-emptive mitigations.

This paper provides details of a study of the structural geology, highly confined aquifer conditions, and a potential collapse column in the Huainan mining area. A three-dimensional prevention and control method (3DPCM) is proposed together with the role of 3D seismic exploration, combined with drilling, to identify the complex geological structures. The effective grouting technology and the stability of a collapse column in the mining process were analyzed by numerical simulation and confirmed by MS monitoring. The necessity of grouting reinforcement is demonstrated along with the stress distribution in response to grouting, so as to provide theoretical support for safe coal mining in areas of deep confined pressurized groundwater.

Project Overview

The Zhangji coal mine of the Huainan Mining Group is located in Anhui province. The mine is composed of three areas: a central area, north area, and air shaft area. The central and north areas adopt the mining mode of zonal development, ventilation, and centralized coal extraction respectively (Fig. 1). The 1612A working face, which is located on the west side of the industrial square in the north area, was mainly mined out by 2018. According to the 3D seismic, surface drilling, and exposure mapping in the mine roadway, the coal and rock strata within the 1612A workings have a monoclinic structure, with some local waviness. The overall dip angle of the rock strata is 8–14°, with an average of 9.5°. The coal strata may be offset by geologic structure. There were 3 faults exposed in the working face, 7 exposed in the belt transportation roadway, and two faults in the drainage lane. The main stratum and production geological conditions of the working face are shown in Fig. 1.

The coal seam mined in the 1612A working face is the 1# coal seam with a thickness of 2.1–9.1 m and an average thickness of 6.3 m. There are composite aquifers of Ordovician limestone and Taiyuan limestone in the coal seam floor. The Taiyuan limestone has three groups (C_3I, C_3II and C_3III), with a total of 12 layers (C_3^{1} C_3^{2} …C_3^{11} C_3^{12}). The average thickness of the coal seam floor aquifuge above the C_3^{1} limestone is about 17 m. The Ordovician limestone water is about 120 m below the coal seam and is an important water source for mining.

According to the exploration results of floor failure in the other working faces, the floor failure of Group A coal may affect the deeper Taiyuan limestone and Ordovician limestone through geological structures. There is basically no hydraulic connection between the Taiyuan aquifer and the underlying Ordovician aquifer (Group) under normal conditions, but if subsidence columns or other water-conducting channels develop in the Taiyuan and Ordovician limestone strata, the confined water may threaten mining of the no.1 coal seam. Therefore, the main water hazards of the 1612A working face floor are the Taiyuan limestone (C_3I, C_3II and C_3III) and Ordovician limestone (Fig. 1b).

Many faults were anticipated to be exposed in the 1612A track and belt transportation roadways during excavation and it was expected that there might be a small amount of water seepage into the excavation, especially near the faults. No water inflow from the pressurized limestone aquifer was expected and there was no large water leakage inflow from boreholes associated with cross layer and directional long drilling. However, targeted measures to prevent limestone water inflows were recommended due to possible disturbance associated with mining. The working face contains two mining roadways, a floor gas drainage roadway, and a floor limestone drainage roadway. As previously noted, the Ordovician limestone could threaten the working face, especially if possible permeable faults or collapse columns release the confined water and cause an inrush.

During the driving and mining period, a 427 m long directional drilling hole (11#) was advanced in the C_3^{3} limestone, along the—600 m drainage roadway of the no.1 coal mining area, as shown in Fig. 1. In April 2018, seepage water was encountered at a depth of about 330 m, and the initial water volume was about 3 m^3/h (Fig. 1b). After all the drill pipes were pulled out, the stable water volume was 220 m^3/h, and the water temperature was 40.5 ℃. The hole was then sealed, and the stable water pressure was measured as 5.9 MPa in the collapse column area. Combined with the measured water quality information, including the pH value, the content of anion and cation, and solid substances, the source was identified as Ordovician limestone water.

Methodology

Since the group A coal seam is threatened by a water inrush hazard from the high-pressure limestone aquifer beneath the coal seam floor, a three-dimensional prevention and control program (3DPCM) from the ground surface was proposed. The drilling from the surface was equipped with geomagnetic detection technology to measure the geological conditions and control the grouting before the mining advanced through the area of concern. Floor damage in the mining area was monitored by drilling drainage exploration holes and installing a microseismic monitoring system (Fig. 2).

3D seismic exploration of the geological structure was used to detect the faults and potential collapse columns of concern and to design surface directional drilling to intercept these features. 3D seismic interpretation was used to layout closely spaced (≤30 m) multi-branch horizontal grout holes. Grouting was carried out in the area of an identified geological anomaly (a potential collapse column) and its surrounding zone of influence, to seal connections to the limestone

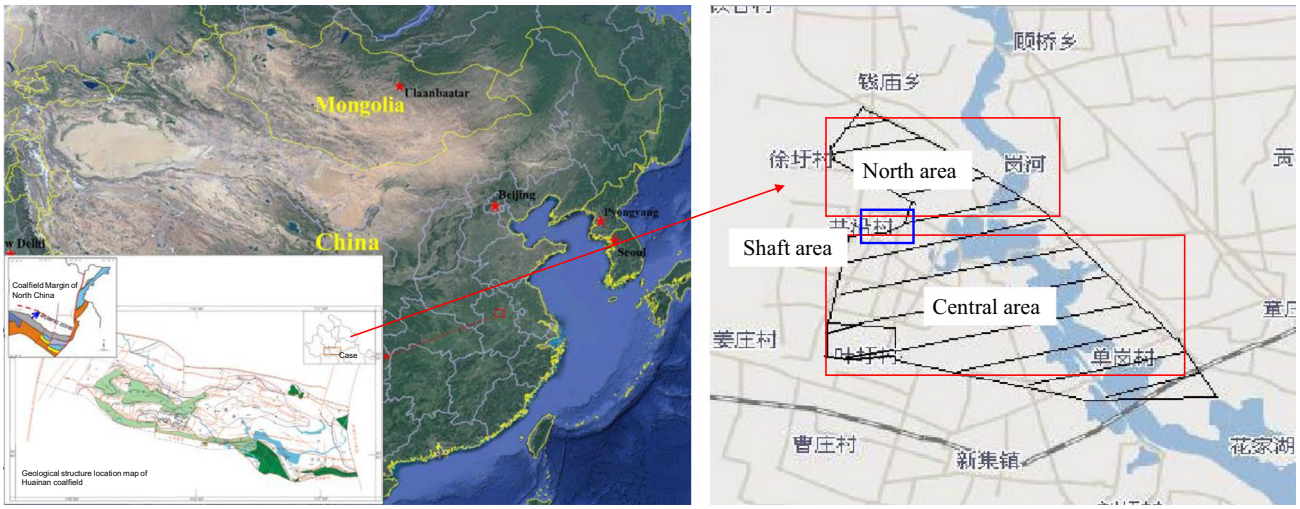

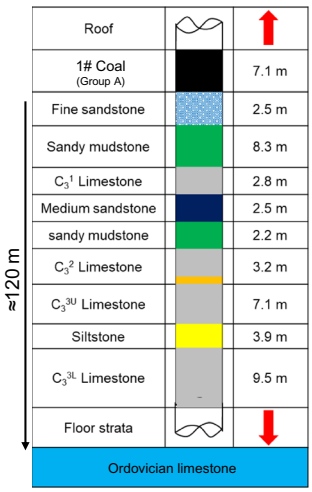

(a) Distribution diagram of floor stratum

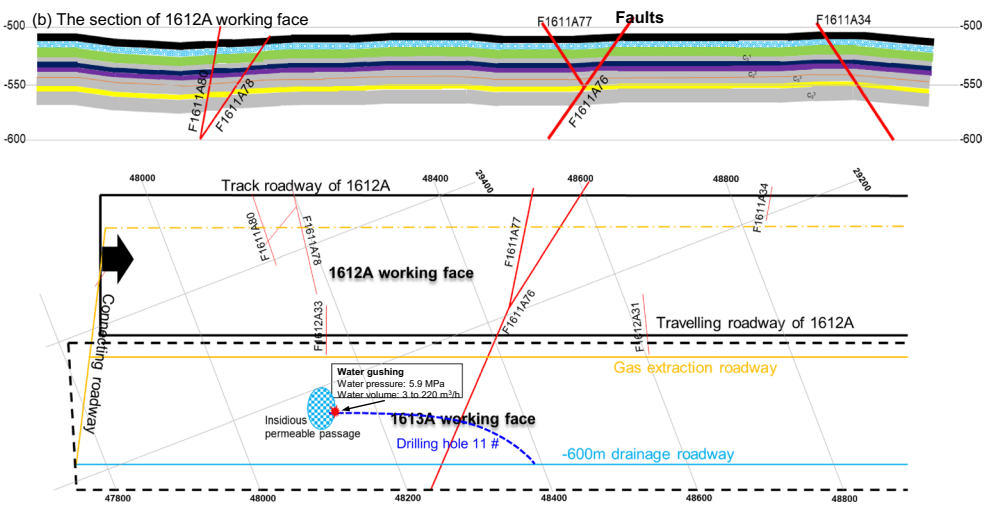

(c) The plan of 1612A working face

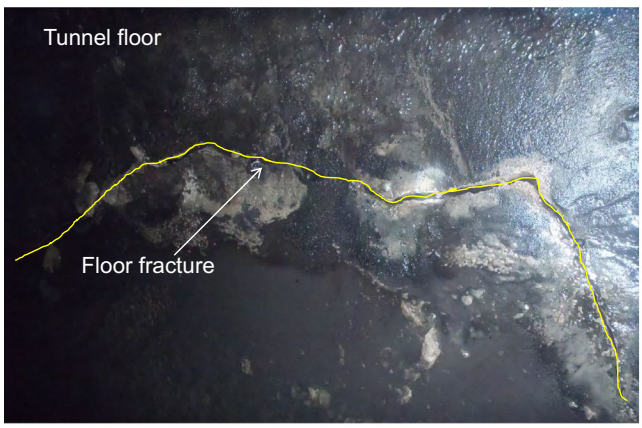

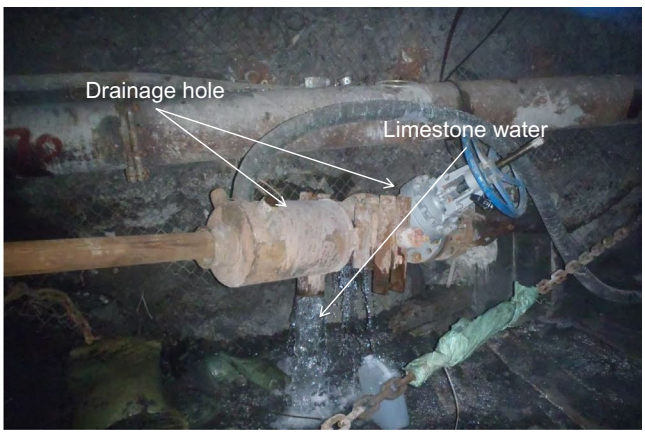

Fig. 1 Engineering conditions

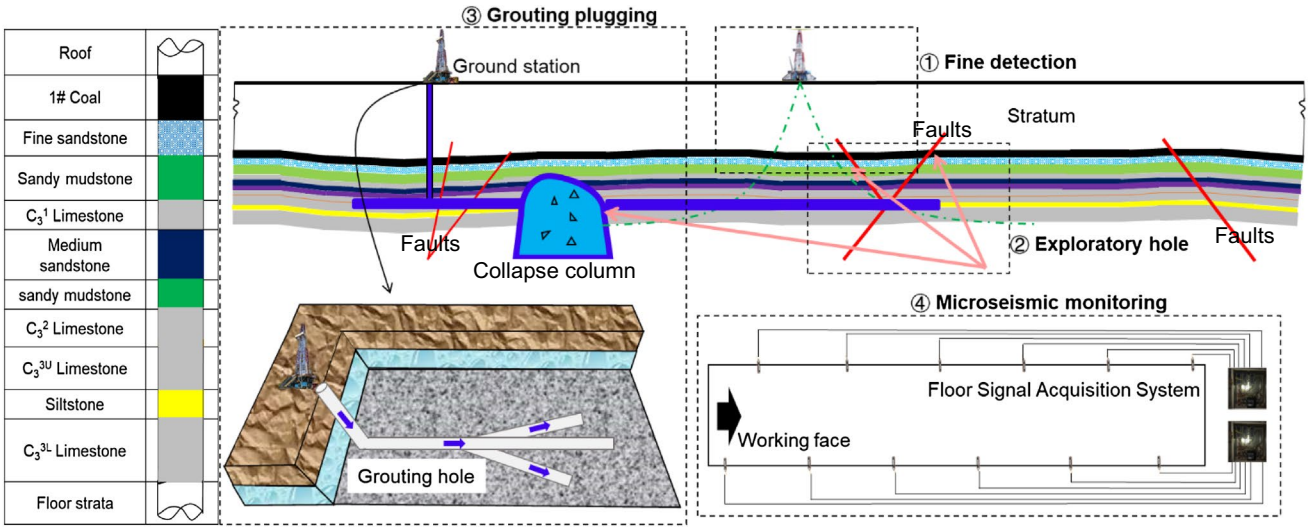

Fig. 2 Schematic diagram of proposed method (3DPCM)

aquifer and control subsequent fracture development. At the same time, MS monitoring was combined with numerical simulation and comprehensive ground response monitoring to verify the performance.

Grouting of the Coal Floor Water Channels

Grouting injects cement slurry under pressure into the fractured rock mass. The slurry displaces the water in the joints/faults and can extend and fill small fractures to achieve effective hydraulic plugging and structurally reinforce the rock mass. Grouting can be done in the karst limestone fractures and in the fractures of the floor rock aquiclude. The grouting method adopted uses horizontal directional drilling, which can be done in three typical geometries:

- In grouting structure 1 (GS1), a main drill hole is used with branches arranged at constant spacing. This has the advantages of a uniform hole distribution, requires little engineering, and has few blind areas, but it has high drilling and injection requirements. This method is called the meridians of leaves type (Fig. 3a).
- In grouting structure 2 (GS2), several horizontal branch boreholes are arranged in parallel from the main vertical holes after drilling the vertical holes from the ground surface to the designated layer. The drilling spacing of this method is uniform, ensuring there is no blind area, but the required engineering and construction are difficult, the coordination of drilling and injection is difficult and must be controlled by parallel distributed branch holes. This is called the fish bone type geometry (Fig. 3b).
- In grouting structure 3 (GS3), the branch boreholes are arranged as a fan from the main vertical holes after the vertical holes are drilled from the ground surface to the designated layer. Multiple boreholes and fans can be used to deliver grout to the main fracture zone (Fig. 3c). This arrangement was used in the collapse column area.

Rock Failure Monitoring from MS Events

Microseismic System in the Working Face

Grouting should be completed based on the design requirements. However, the penetration of grout slurry into the fractured rock body is affected by many factors, such as in-situ stress and fracture geometry. Due to these unknowns, grouting may not always achieve the required water sealing and/or rock strength improvements. Moreover, effective grouting needs to ensure stability as the rock mass responds to mining excavation; therefore, to maintain safety, it is necessary to monitor the excavation-induced damage of the surrounding rock in real time. Stress concentration and energy accumulation occur in the rock mass as the external load changes due to the mining process. When the external load stress concentrations exceed the ultimate strength of the rock, damage and ultimately failure of the rock mass can be induced due to the initiation and propagation of cracks in the rock mass. Energy will be released in the form of stress wave as cracks form and propagate, resulting in MS events. MS technology can be used to monitor the P waves and S waves generated by rock fracturing and identify their locations (Cheng et al. 2019). As shown in Fig. 4, events measured at carefully located sensors, arranged in staggered space in the

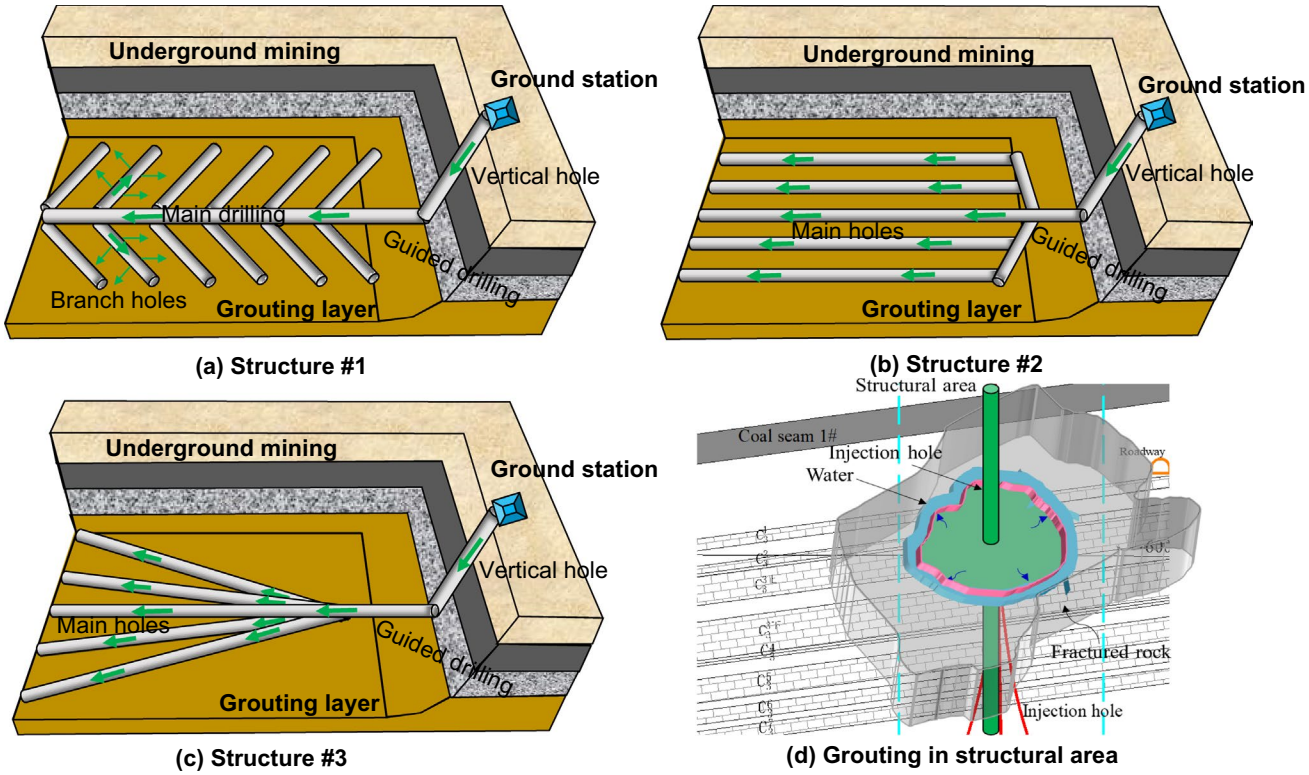

Fig. 3 Grouting in coal floor

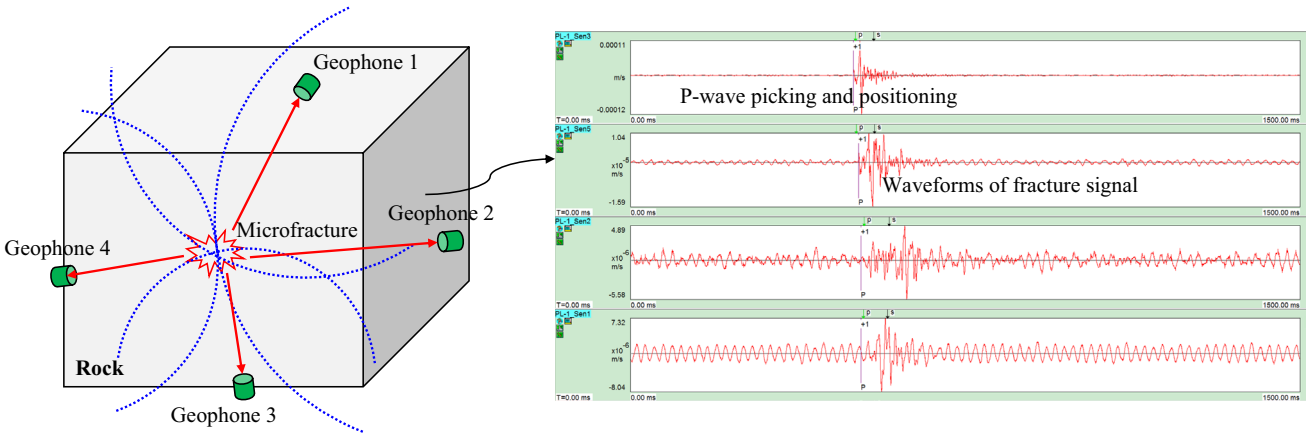

Fig. 4 Microseismic monitoring technology under rock fracture

rock mass, especially in the vertical direction, can be used to calculate the time difference of a waveform received by four or more sensors. Each MS event represents potential damage and failure of the rock mass. The location of the MS events gives an indication of the depth and extent of damage to the floor rock. Based on the temporal and spatial characteristics of the MS identified microfractures, the activity zone, stability, and developmental trend of rock mass failure can be evaluated (Zhou et al. 2017).

MS events deliver different signatures in different rock layers and as the state of the rock changes in response to fracturing in the coal floor, allowing the user to assess accumulated damage in the area and the trend towards macro-failure of the rock mass. The water inrush development often shows temporal and spatial characteristics in the monitored MS. Based on the "down three zone" theory (Shi et al. 2020), a common failure sequence is when the fracture zone extends downward deeply, and the confined water

pressure causes upward fracture propagation. Water inrush is caused by the connection of upward and downward propagating fracture zones. The temporal and spatial distribution characteristics and evolution trend of floor failure obtained from the MS information is essential to the effective evaluation of floor safety. Therefore, an ESG MS monitoring and centralized analysis system (ESG Solutions Kingston, Ont. Canada) was used to continuously monitor the 1612A working face to locate and analyze fracture development and infer the risk of water inrush. A rock bolt was constructed in a 45° inclined hole in the side wall of the roadway, and the microseismic signal sensor was attached to the bolt using a sleeve whose internal diameter is slightly larger than the diameter of the sensor. The sleeve was welded at the end of an anchor rod. The sensor is inserted into the sleeve for tightening and fixing.

As shown in Figs. 5, 12 sensors were arranged in each roadway, and the sensors were fixed on the two sides of the roadway using bolts, as described. The distance between adjacent installation monitoring points is 100 m. First, 12 sensors were installed on the bolts of the no. 1–6 and no. 13–18 installation points respectively to monitor the early mining signal. When the working face had advanced to 550 m, the sensors at installation points 1–3 and 13–15 were transferred to installation points 7–9 and 19–21. When the working face had advanced to the position of 850 m, the sensors at installation points 4–6 and 16–18 were transferred to installation points 10–12 and 22–24.

Verification of MS Monitoring

The MS monitoring system has been widely used and is effective and reliable for monitoring rock mass damage and mine water disaster prevention and control (Cheng et al. 2021a, b, c; Ma et al. 2021). The monitoring results are highly consistent with the floor failure depth predicted for the site (Cheng et al. 2021a, b, c). In the process of field monitoring, background noise can be eliminated based on the spectral characteristics, allowing the rock fracture waveform to be identified. To verify the parameters for the MS monitoring system, five blasts were carried out in the stope, and the wave arrival times were recorded to verify the geophone response and positioning (Table 1). The blasting time and calculated spatial position were in good agreement with the surveyed installed positions, with a positioning error of ± 5 m.

Results

Geological Exploration

The interpretation of the 3D downhole seismic test is shown in Fig. 6. The section on the top left shows pre-stack time migration; the area below the seepage points in directional hole (red dotted ellipse) #11 shows weak bending and amplitude weakening characteristics. The anomaly is easy to miss because of the small variation relative to the background signals. The top right of Fig. 6 shows a later section of pre-stack depth migration; the same position inside the red ellipse shows a more obvious in-phase depression. Through detection of sensitive seismic attributes, a potential collapse column was identified. Our interpretation of the restack depth migration profile shows an anomaly in the area below the borehole 11# seepage area. Additional signal processing, shown in the lower half of Fig. 6, from left to right presents

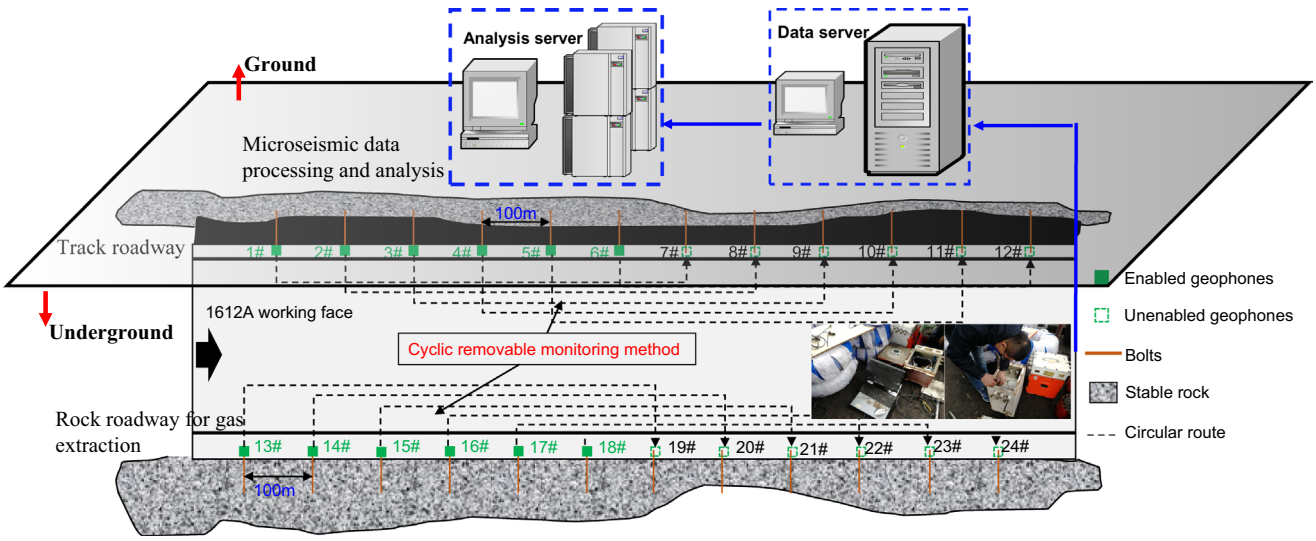

Fig. 5 Microseismic system in 1612A working face

Table 1 Calibration of microseismic monitoring

Waveform data acquisition

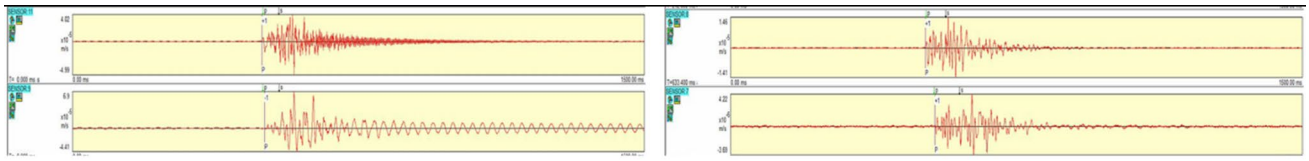

Rock failure waveform

Positioning results				Field measurement results		
Time	X	Y	Energy/J	Time	X	Y
2019-3-1 19:05	29,413.71	48,141.75	2.38E + 04	2019-3-1 19:05	29,413.71	48,142.13
2019-3-1 22:19	29,309.43	48,044.29	9.23E + 03	2019-3-1 22:20	29,305.82	48,039.03
2019-3-2 20:12	29,244.1	48,148.05	1.12E + 04	2019-3-2 20:12	29,241.8	48,145.23
2019-3-2 23:58	29,297.76	48,036.86	1.05E + 04	2019-3-2 23:57	29,292.98	48,031.35
2019-3-7 22:28	29,272.15	48,054.96	1.27E + 04	2019-3-7 22:29	29,277.01	48,050.17

Positioning results from MS monitoring was consistent with the field measurement

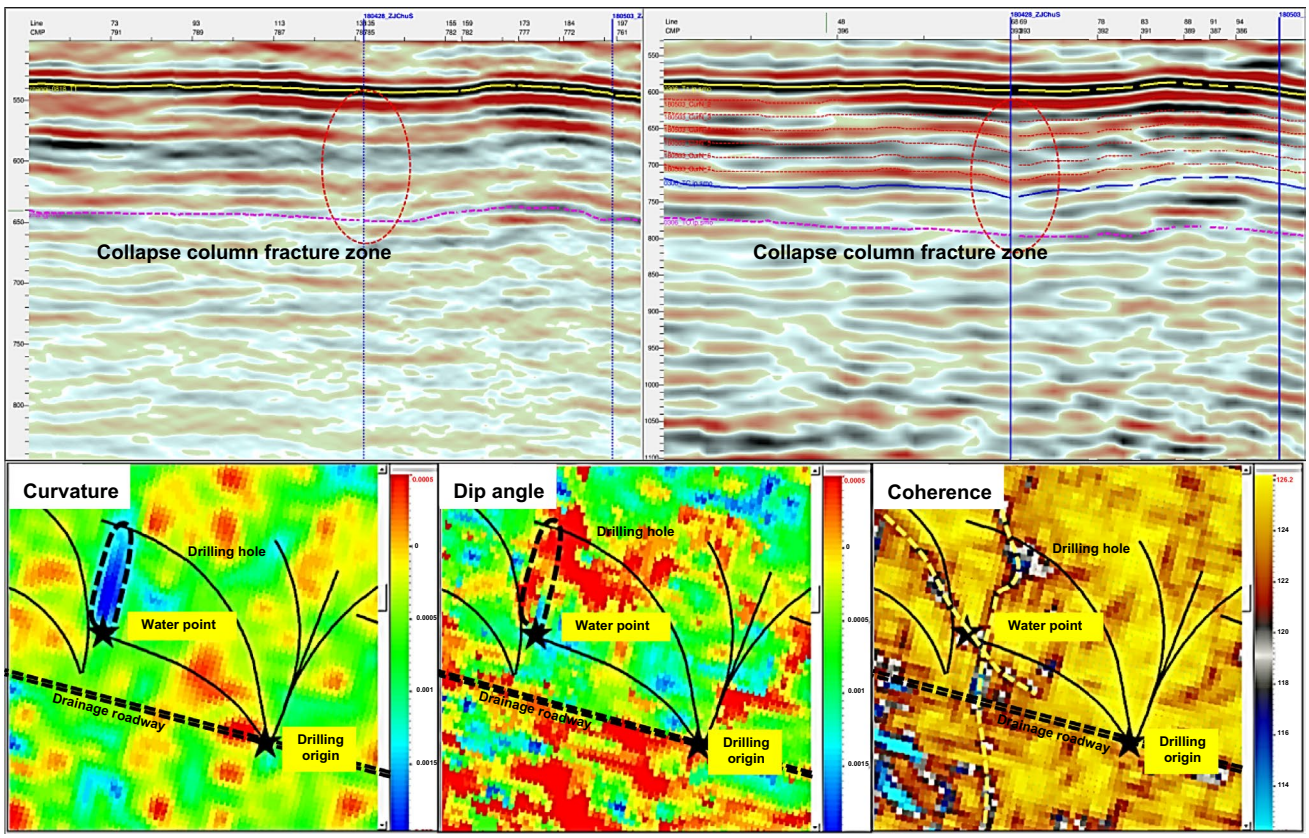

Fig. 6 Seismic migration profile along the track of directional hole

the maximum negative curvature, the maximum dip angle, and the minimum coherent anomalies (Marroquin et al. 2004; Zhou et al. 2020; Zuo et al. 2009). This phenomenon shows that in the noted seepage area, the continuity of strata is poor and there may be geological anomalies. According to the seismic multi-attribute detection results, the northern

part of borehole 11# seepage is located adjacent to an elliptical maximum negative curvature attribute anomaly area (left-most bottom figure). The low value of the minimum coherence attribute anomaly shows an "X" intersection (right), which is suspected to be a conjugate shear fault.

According to the monitoring results from the mine workings, it was inferred that there is local ground subsidence related to the conjugate shear fault identified in Fig. 6. This anomaly is suspected to be a developing collapse column fracture zone. Further drilling revealed that there was a thin fault zone at a depth of about 53 m that appears to be able to conduct water and could be the site of a future water inrush. In this area, the fractures are distributed in blocks and are closely connected with the lower fault zone. With further drilling exploration to verify the original borehole data and the multi-attribute interpretation of 3D seismic data, namely coherence, curvature, dip angle, phase and texture, a developing elliptical collapse column with a length of 53 m and a width of 35 m was delineated (Fig. 6).

Multistage High-Pressure Segmented Grouting

Given the geological conditions and the water pressure in the underlying aquifer, a multi-stage segmented high-pressure grouting method (GS3, Fig. 3) was designed to provide a seal for seepage and to reinforce the detected potential collapse column (Ren et al. 2021). Based on the geological conditions in the stope, a main grouting hole; two branch grouting holes were drilled. The detected seepage zone in the no. 11 borehole drilled from the -600 m level drainage roadway was in the C_3^3 lower limestone, and the seepage source was confirmed to be derived from Ordovician limestone water, based on water quality. Therefore, the main grouting target was determined to be the C_3^3–C_3^{11} limestone layer. A design criterion for effective grouting was determined; limiting single hole seepage to less than 3 m^3/h would sufficiently control seepage and water inrush.

The plan layout and branch holes are shown in Fig. 7. The designed radius of grout penetration was 30 m, with the boreholes spaced 15–25 m apart. The ends of all grouting holes were arranged close to the base of the potential collapse column to ensure that the main fracture zone was properly grouted. Each main grout hole has at least two secondary grouting holes (Fig. 7), arranged to achieve the required area of grout penetration. Grout flows predominantly along the existing fractures, with limited penetration into the intact rock. Consequently, grouting stages were selected in different layers at different depths. In this way, areas missed by a single grouting hole can be covered by grouting in other layers, so as to complete the regional reduction in rock permeability.

Figure 8 shows cross sections of the grout holes. The main hole, IH-1, is a straight hole with a depth of about 716 m and a hole bottom elevation of – 694 m, which is in the lower part of the C_3^{11} limestone. Hole IH-2 is located north of the main hole and had a depth of about 677 m; the elevation of the hole bottom is -655 m, which is in the C_3^9 limestone. Hole IH-3 is located south of the main hole in the depth range of C_3^6-C_3^9 (Ren et al. 2021). Directional drilling was used to position the grouting section of the holes within the identified, potential collapse column and at a spacing required to complete the sealing and strengthening of the collapse column, assuming a grout penetration radius of 30 m.

Before grouting, a water injection test was carried out to measure water pressure and to estimate grout take in the

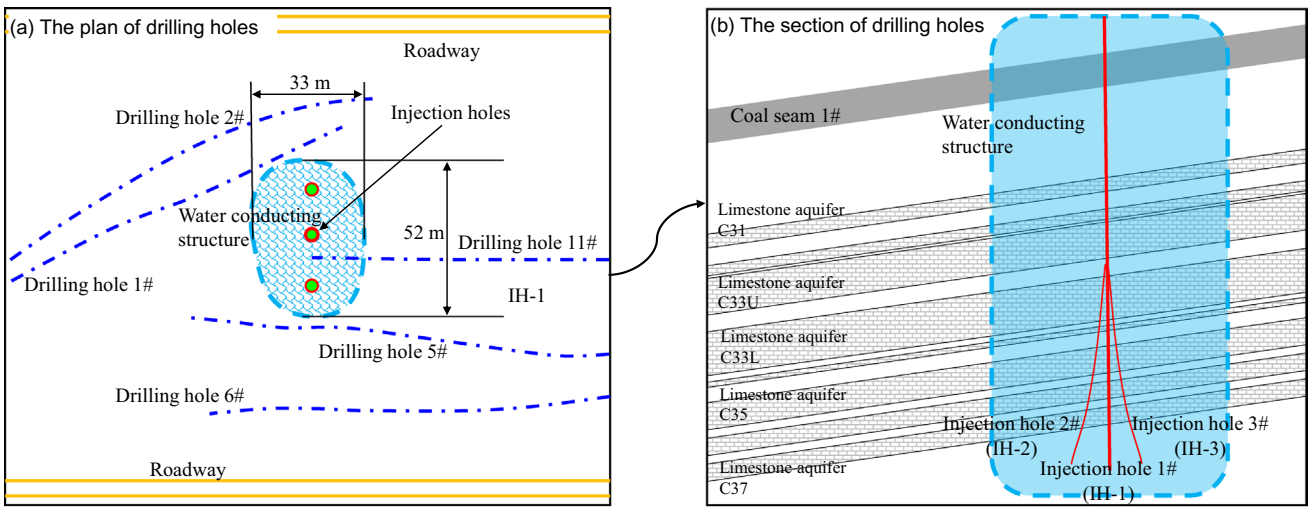

Fig. 7 Spatial position of grouting and verification holes in working face

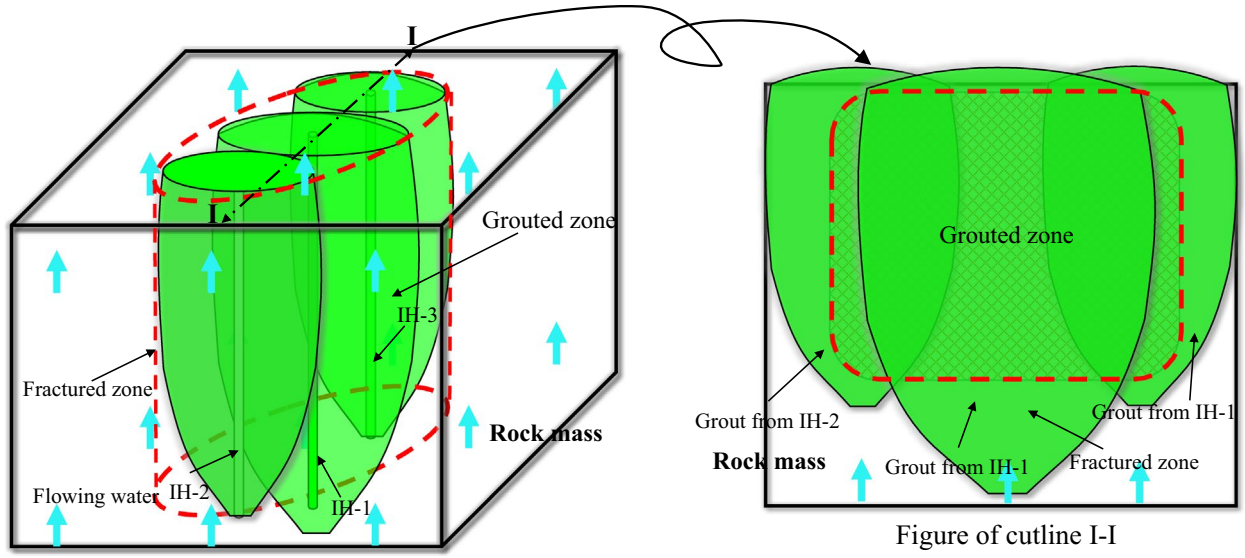

Fig. 8 Grouting flow in the rock fractures at the key layers (Ren et al. 2021)

target zone The grouting methods included whole section grouting, limited multi-stage grouting, and multi-stage grouting based on water pressure testing. The slurry was diluted first and then progressively thickened, and the interval of intermittent grouting was less than 12 h between grouting campaigns. The idealized zone of grouting is shown in Fig. 8; under the action of water flow and grouting pressure, the slurry diffuses in the fracture area to achieve plugging and reinforcement.

Figure 9 shows the real-time observation of seepage from hole H-11# after the grouting; the seepage flow decreased in response to multiple grouting injections (from 7 m^3/h to 0). Verification hole TH-1# also showed minimal seepage after grouting.

Rock core within the grouted horizons was obtained from drill holes in the drainage roadway to further verify the grouting in the floor rock mass, as shown in Fig. 9. It can be seen that the fractures in the rock mass were filled with cement, and the broken rock had its permeability decreased and was strengthened by the cement slurry. According to previous research (Ren et al. 2021), initial grouting from the main hole achieves preliminary plugging in the dominant fractures first. Then, as water seepage and pressure decrease, the slurry diffuses into secondary fractures to fill and block the whole area. Therefore, after grouting, it can be seen from the coring that the floor rock is in a relatively stable state.

However, subsequent mining in the 1612A working face, an adjacent stope, is expected to create stress changes in the rock that could disturb the grout stabilized rock of the collapse column. This disturbance could potentially create a connection between the collapse column and the confined pressurized groundwater and cause a secondary water inrush accident. Therefore, the MS monitoring system was built during 1612A mining period to monitor the stability of the grouted potential collapse column.

Damage and Failure of the Rock Surrounding the Collapse Column

The MS monitoring system has been operating in the mine since the end of February 2019. The monitoring focuses on the grouted area from near the potential collapse column to the end of working face, shown as the mining line in Fig. 10, which also shows the location of the potential collapse column (red ellipse) and grouted rock in the stope. By analyzing the distribution of MS events in the rock surrounding the coal seam, it can be seen that the disturbance caused by coal mining affects the adjacent stope, including the collapse column area. MS events are widely distributed in the non-grouted areas (e.g. sections I–I and III–III), suggesting some regional micro-fracturing in the rock. However, in the location of the grouted zone (II–II), there were no MS events recorded, which indicates the improved stability of the grouted rock.

To analyze the mining disturbance, the number of MS events in the floor within radius distances from 10 to 100 m from the center of the grouting zone was obtained (Fig. 11). A significant reduction in the frequency of MS events within 60 m of the grouted zone can be seen. Section III–III had the greatest activity, which is thought to be due to a fault identified in that area. However, section III–III still shows reduced activity within 60 m of the grouted zone. Sections I–I and II–II show similar reductions in activity within 60 m

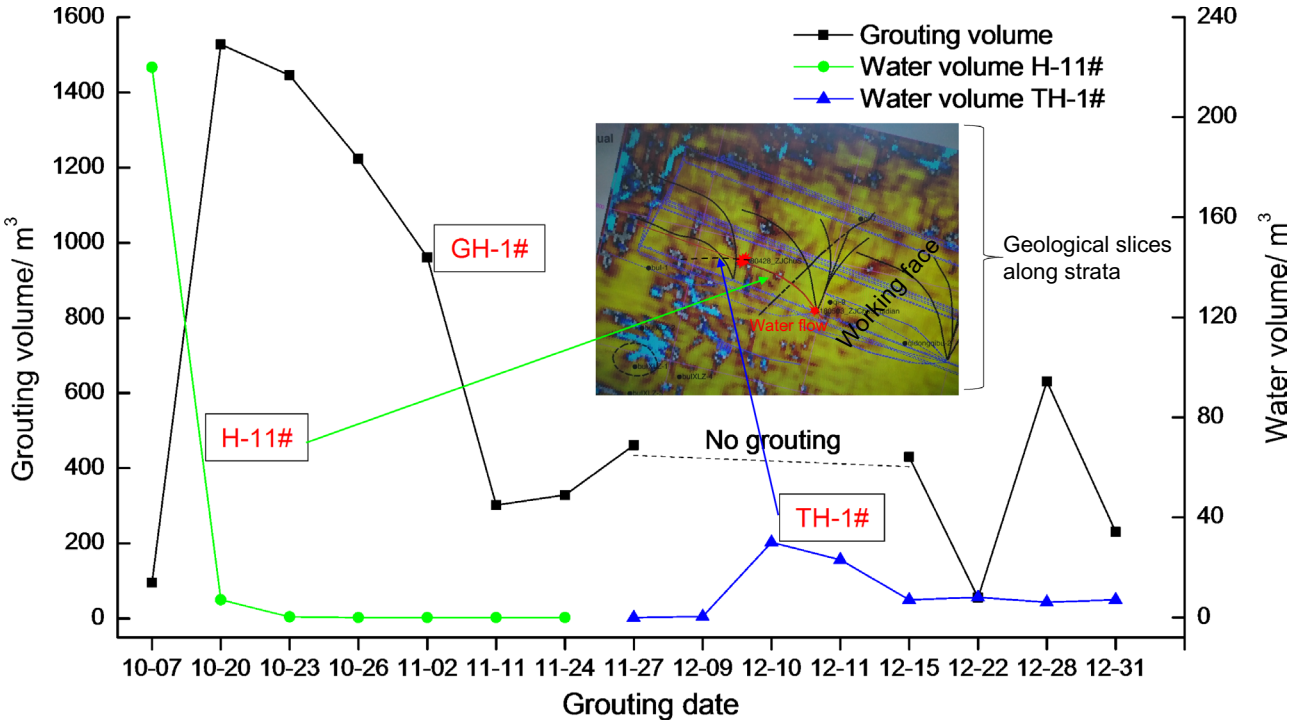

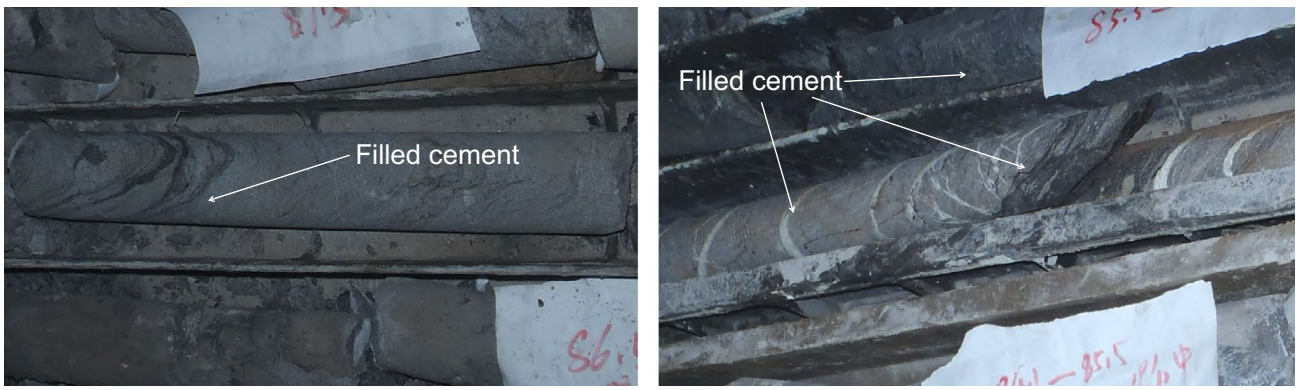

Fig. 9 Grouting in coal floor

of the grouted zone; activity increases beyond 60 m and the three sections show similar microseismic activity near the working face.

Numerical Calculation

A numerical model was set up to attempt to reproduce the measured response of the rock to stress changes due to mining. Some strata are simplified and combined, and the numerical model was established for discussion and analysis based on the FLAC3D software, as shown in Fig. 12. The model is 600 m long × 600 m wide × 400 m high. The dip angle of the strata is about 10°, and the size of the fracture zone is 52 m long × 33 m wide. The stress disturbance of the potential collapse column was simulated based on the Mohr–Coulomb criterion, as mining progressed.

The geo-mechanical parameters of the main strata were obtained from the well geophysical logging data and the laboratory core performance test (provided by the mine). The physical and geo-mechanical parameters of rock mass used in the numerical model are illustrated in Table 2.

First, to verify the accuracy of the numerical model, the calculated rock stress was compared with the field monitoring data at different advancing distances of the simulated stope at five collection sites. The pressure of the aquifer was modeled by applying permeation stress to the numerical stratum. The vertical stress value of each monitoring

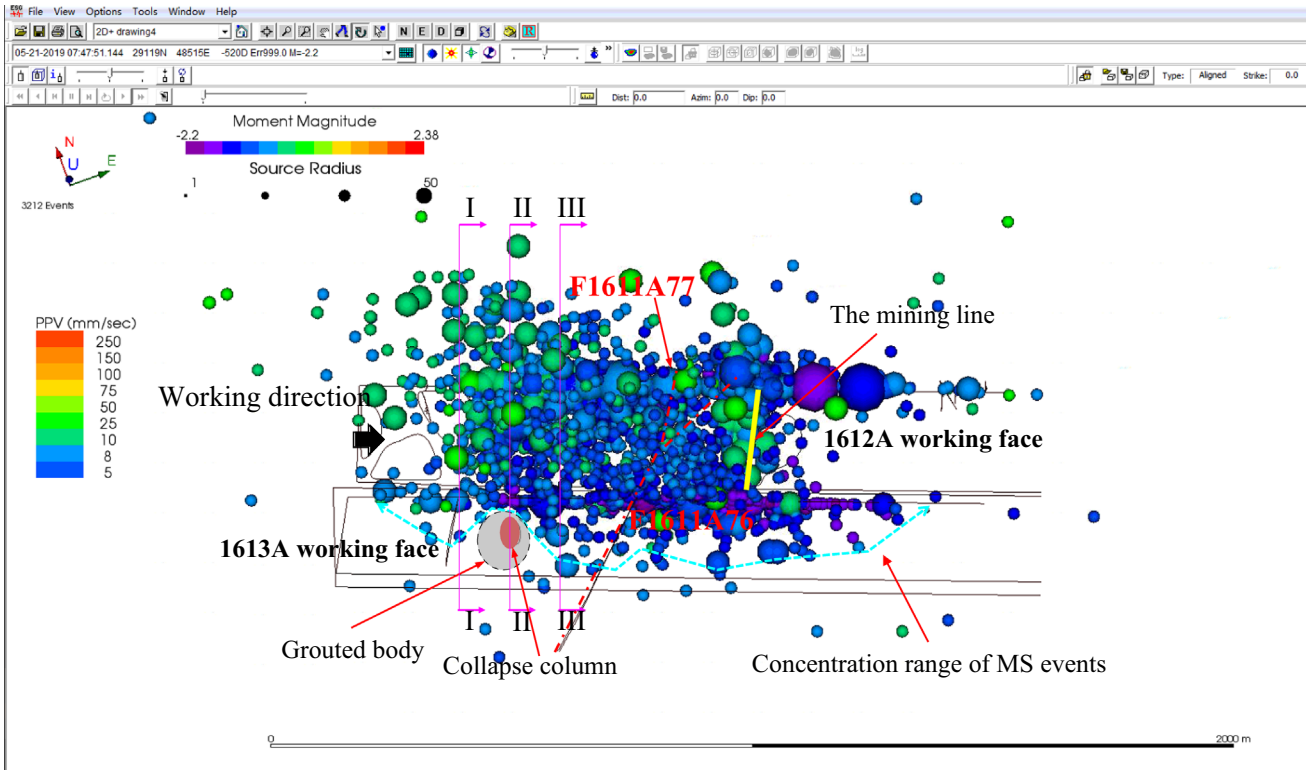

Fig. 10 MS events in stope

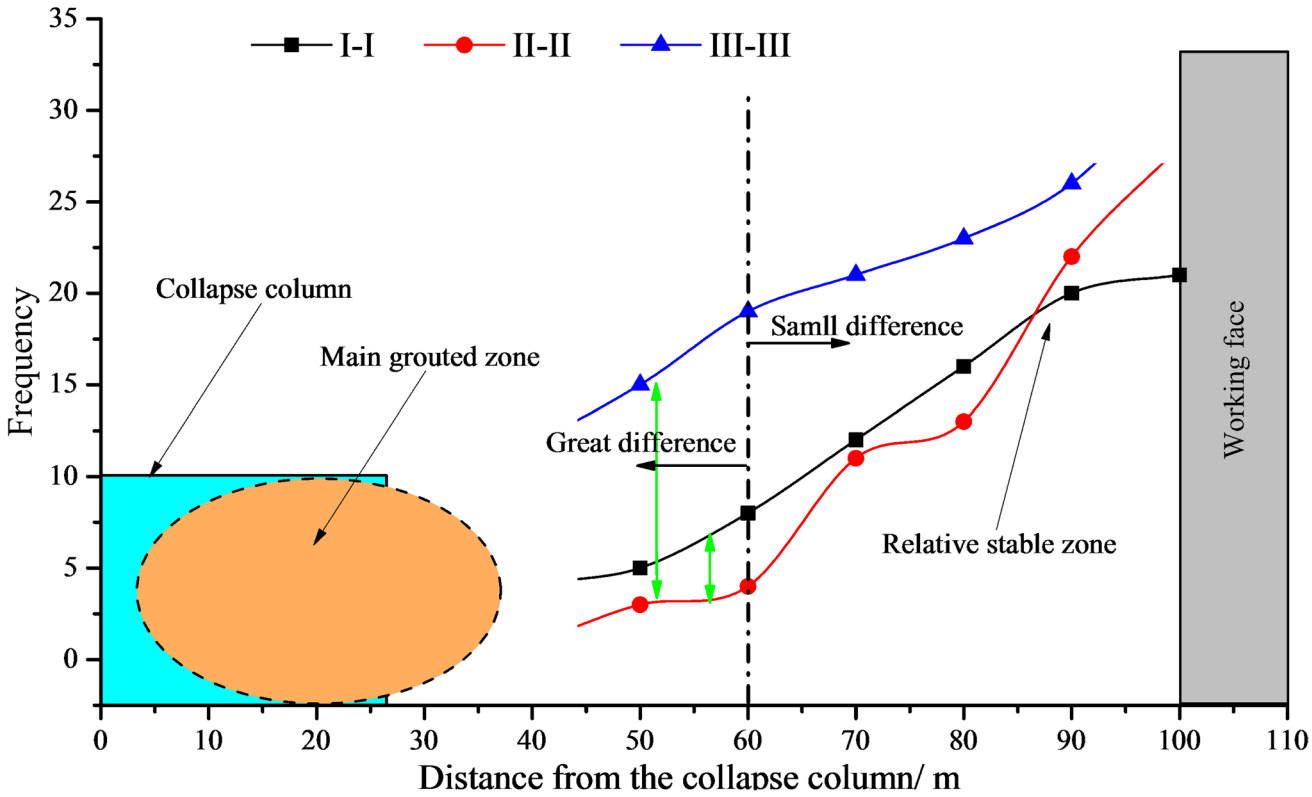

Fig. 11 Frequency of the MS events along the distance

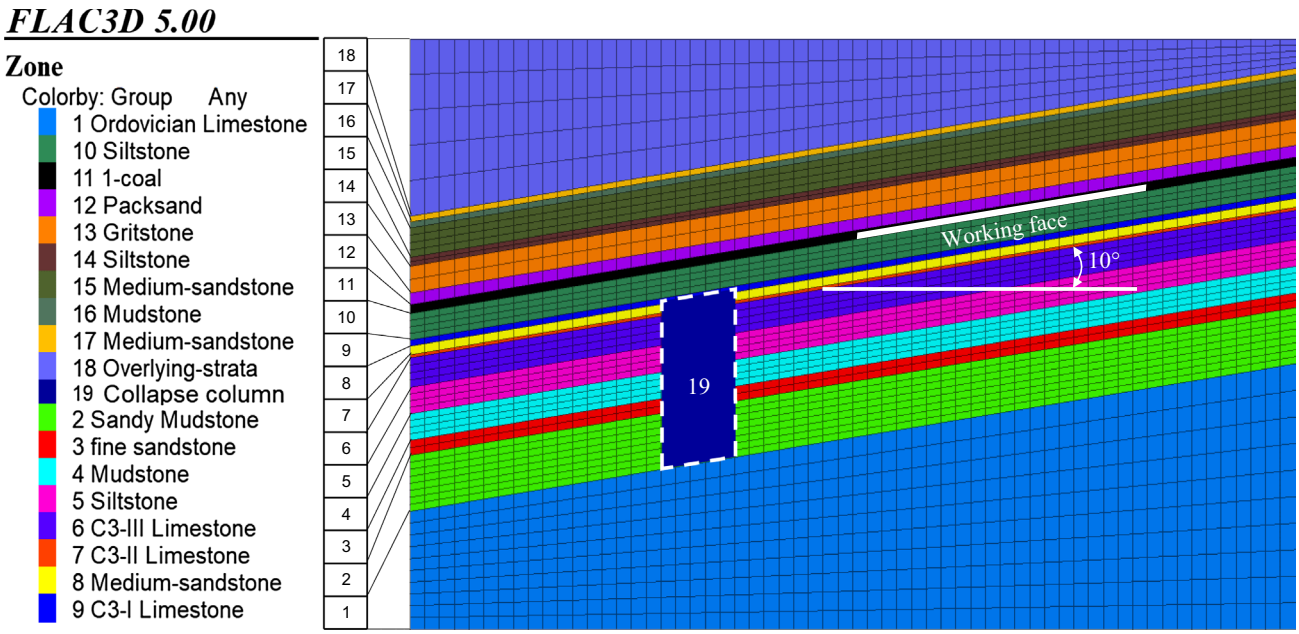

Fig. 12 Numerical model

Table 2 Mechanical parameters of rock mass

Rock strata	Density/kg/m^3	Bulk modulus/GPa	Shear modulus/GPa	Friction angle	Cohesion/MPa	Tensile strength/MPa
Limestone	2770	10.42	10.42	35.8	8.80	4.45
Medium Sandstone	2666	9.44	3.86	57	7.98	7.8
Mudstone	2533	9.53	4.99	34.9	2.20	1.45
Sandy mudstone	2760	11.36	6.18	35	14.5	4.6
Siltstone	2533	9.53	4.99	34.9	2.20	1.45
Coal	1450	1.25	0.58	30	0.8	0.3
Collapse column	1300	1.05	0.35	18	0.35	0.13
Grouted zone	2533	10.2	5.02	39	3.2	2.45

point (numerical calculations #1, #2, #3, #4, #5) in the middle of the stope was extracted from the FLAC3D numerical simulation results; the changes with mining advancement are plotted in Fig. 13. It can be seen that the rock stress surrounding the stope reaches a peak value and then declines after the working face continues its advance. The numerical simulation follows the same trend, indicating that it agrees well with the measured values, thus verifying the model and parameters.

The Flac model identified the distribution of plastic zones in the rock stratum under grouted and non-grouted conditions (Fig. 14). Comparing the two conditions, the rock mass in the area shows opposite states. After grouting, the surrounding rock is relatively stable. In the absence of grouting, seepage pressure from the confined water leads to plastic failure of the potential collapse column and its surrounding rock (Fig. 14a, b). After mining, the modelled plastic zone further develops and connects to the confined aquifer. The analysis shows that grouting effectively eliminates the plastic zone in the collapse column and surrounding rock. The numerical results are consistent with the MS monitoring from Fig. 14, providing mutual verification. The grouted zone changes the spatial distribution characteristics of MS events, consistent with the measured seismic activity, and limits the damage within the grouted area and surrounding rock.

To further understand the stress field changes in the collapse column before and after grouting, the stress distribution during progression of the working face was also modelled by FLAC analysis. Three stress state diagrams of 1612A working face were obtained when: (1) the strata in the working face was 40 m in front of the grouted potential

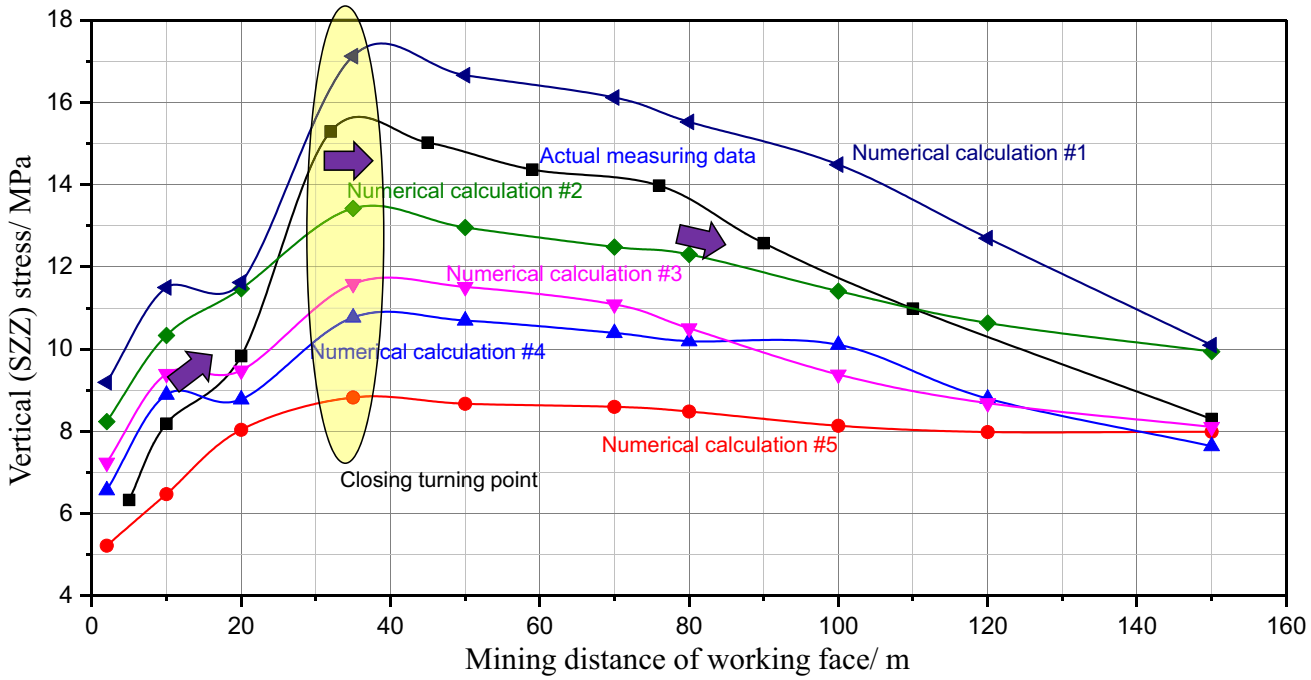

Fig. 13 The variation of stress

collapse column; (2) the working face was adjacent to the grouted potential collapse column; and (3) the working face was 40 m beyond the grouted potential collapse column (Fig. 15). When the working face was mined within 40 m of the potential collapse column, there will be a large abnormal area of stress disturbance. This disturbance can induce damage to the rock stratum. Under the condition of no-grouting, the extremely weak geo-mechanical parameters of the collapse column led to the model-predicted abnormal stress in this area. The modelled predicted vertical stress in the collapse column was low, below 8 MPa, and about 12 MPa less than in the surrounding rock. The low stress is due to shedding of stress to the stronger surrounding rock. After grouting, the grouted zone is coupled with its surrounding rock and the low stress zone does not develop. Due to the reduction of regional stress redistribution and strengthening of grouted rock, the MS events would be expected to be reduced; this agrees with the monitored performance, as shown in Fig. 14(b).

Conclusion

The existence of fractured geologic strata and the underlying pressurized confined aquifer creates a serious potential water in rush hazard. This paper described the mitigation design and treatment of a potential collapse column structure in the mining of group A coal using the 3DPCM approach.

An elliptical anomaly area (a potential collapse column) was found using 3D seismic exploration. An in-phase depression near the anomalous area confirmed the existence of the potential collapse column. Combined with the interpretation of the multi-attribute 3D seismic data and drilling exploration, an elliptical potential collapse column with a length of 53 m and a width of 35 m was delineated. A high-pressure grouting method was designed and implemented to seal and reinforce this elliptical feature. Post-grouting coring verified that the grout slurry had penetrated into the specified region. Grouting resulted in reduced water pressure in the area as the connection to the underlying pressurized aquifer was sealed off. This confirmed the effectiveness of the grouting and reduced the risk of a water in rush event.

The spatiotemporal distribution of rock failure, as mining progressed, was monitored in real time using a MS monitoring system. The greatly reduced MS activity in the grouted region confirmed the effectiveness of the grouting. The results of numerical calculation and MS monitoring agreed, both showed a reduction in the plastic and tensile failure regions in the grouted rock. The geo-mechanical parameters in the grouted region exceed the strengths of the host rock.

The numerical analysis and the MS monitoring confirmed the need for grouting and verified the effectiveness of the grouting program. Grouting reduced the development of both upward and downward fractures and prevented the pressurized aquifer water from reaching the mine, and hence prevented a water inrush disaster.

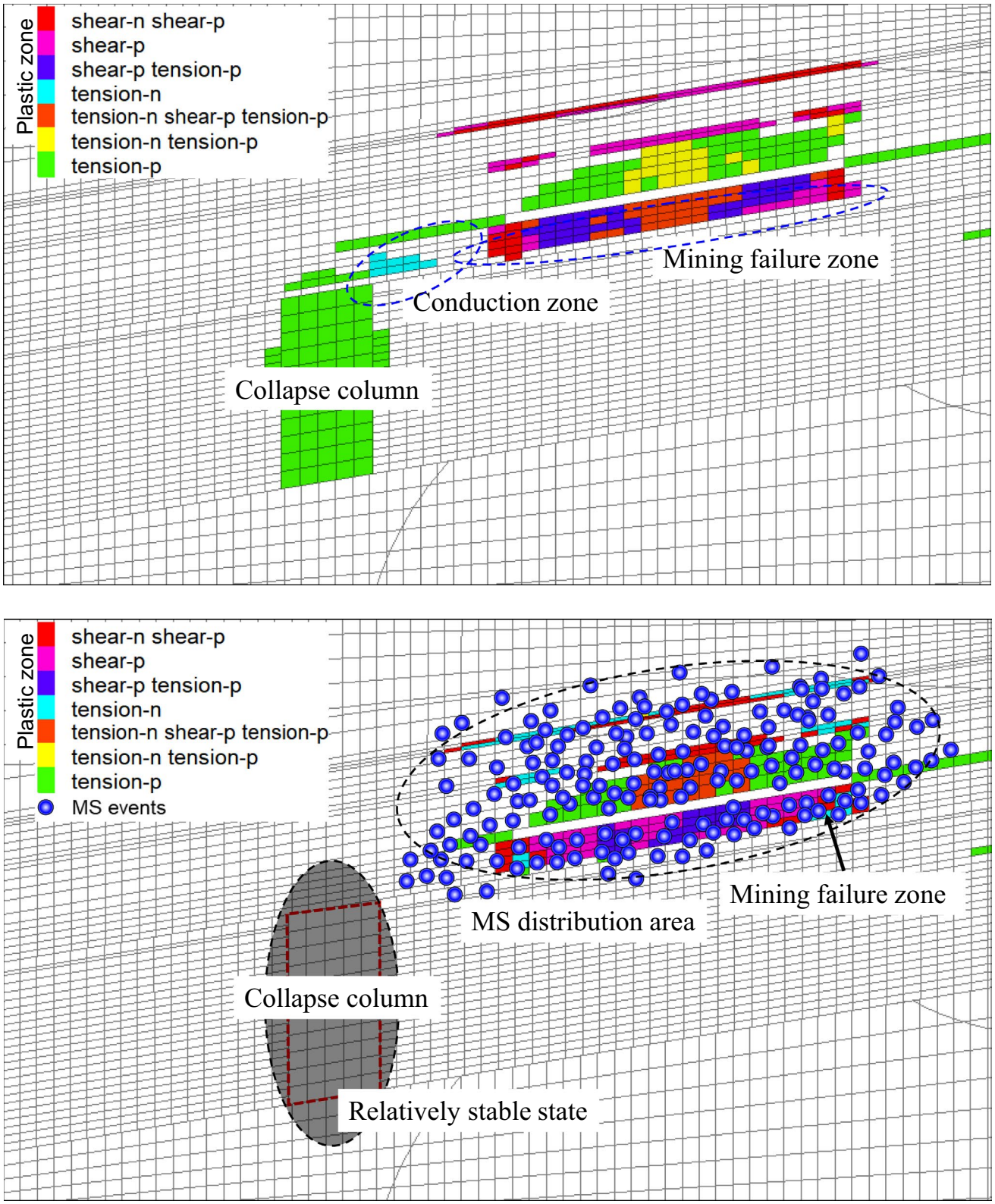

Fig. 14 Distribution of plastic zone in working face after mining

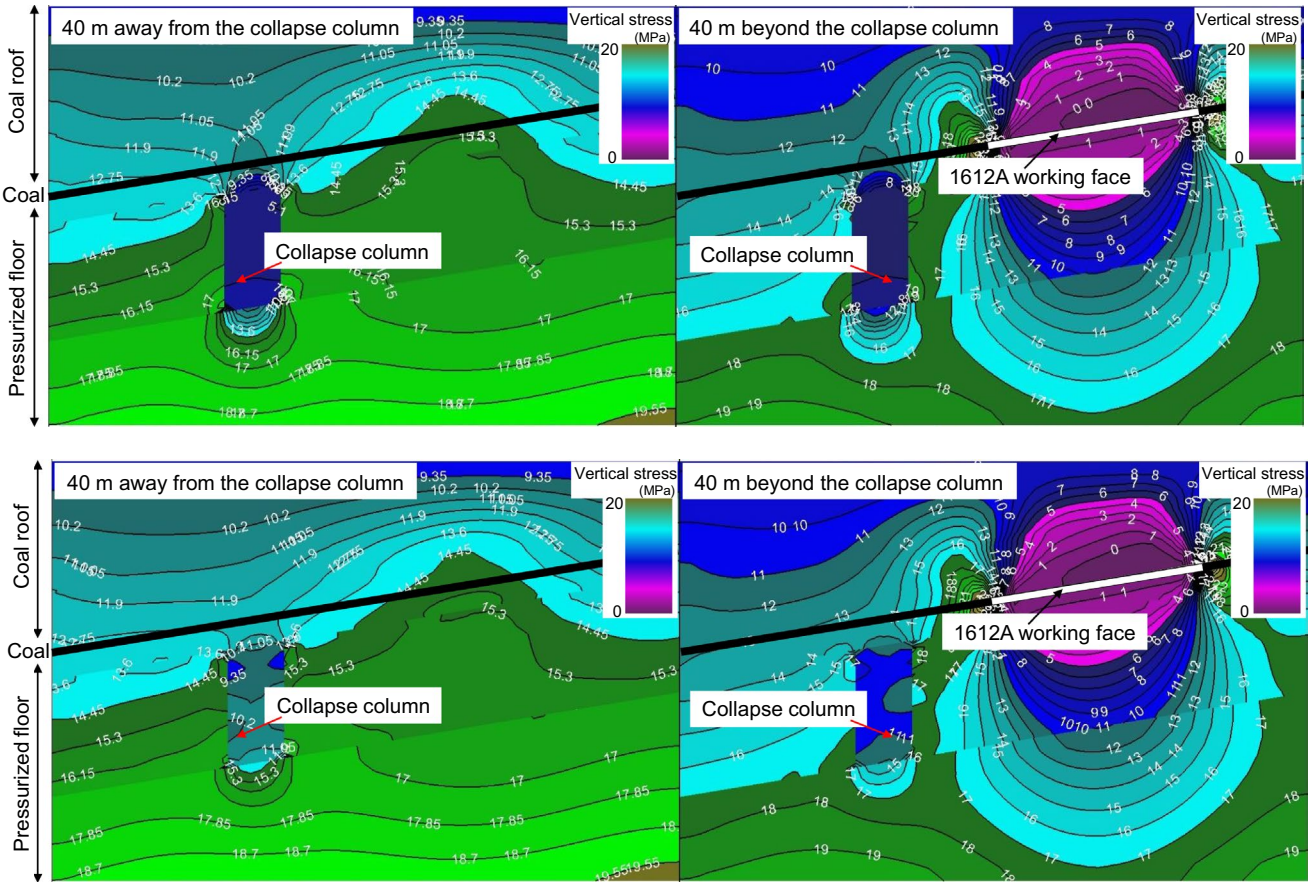

Fig. 15 Stress distribution in coal mining

Acknowledgements This work was conducted with support from the Natural Science Foundation of Anhui Province (2108085QE209), the National Natural Science Foundation of China (Grant 51879041), the Natural Science Foundation of Anhui Province (2008085ME145), and Key Research and Development Plan of Huainan City (2021A05).

Data Availability Some or all data, models, or code generated or used during the study are available from the corresponding author by request.

References

Cheng GW, Li LC, Zhu WC, Yang TH, Tang CA, Zheng Y, Wang Y (2019) Microseismic investigation of mining-induced brittle fault activation in a Chinese coal mine. J Rock Mech Min Sci 123:104096

Cheng AP, Gao YT, Liu C, Chai JF (2021a) Microseismic monitoring and numerical simulation research of floor failure depth in extra-thick coal seam. Adv Mater Res 881–883:1799–1804

Cheng GW, Tang CA, Li LC, Chuai XY, Yang TH, Wei LK (2021b) Micro-fracture precursors of water flow channels induced by coal mining: a case study. Mine Water Environ 40(2):398–414

Cheng JY, Wang P, Nan SH, Qin S (2021c) Rapidly locating a water-inrush collapse column in a seam floor: a case study. Mine Water Environ 40(2):389–397

Chuai XY, Teng JW (2017) Water inrush mechanism research of strong conducting (water including) karstic collapse column. Chin J Geophys-Chin Ed 60(1):430–440

Dong SN, Zhang WZ, Zhou WF, Chai R, Wang H, Zhao CH, Dong XL, Wang QM (2021) Discussion on some topical issues of water prevention and control in coal mines. Mine Water Environ 40(2):547–552

Duan HF, Zhao LJ (2021) New evaluation and prediction method to determine the risk of water inrush from mining coal seam floor. Environ Earth Sci 80(1):30

Hu WY, Zhao CH (2021) Evolution of water hazard control technology in China's coal mines. Mine Water Environ 40(2):334–344

Hu YB, Li WP, Liu SL, Wang QQ (2021) Prediction of floor failure depth in deep coal mines by regression analysis of the multi-factor influence index. Mine Water Environ 40(2):497

Jin DW, Zheng G, Liu ZB, Liu YF, Pang XQ (2011) Real-time monitoring and early warning techniques of water inrush through coal floor. Procedia Earth Planet Sci 3:37–46

Jin DW, Zheng G, Liu ZB, Chen BH (2021) Real-time monitoring and early warning of water inrush in a coal seam floor: a case study. Mine Water Environ 40(2):378–388

Li CP, Li JJ, Li ZX, Hou DY (2013a) Establishment of spatiotemporal dynamic model for water inrush spreading processes in underground mining operations. Saf Sci 55:45–52

Li T, Mei TT, Sun XH, Lv YG, Sheng JQ, Cai M (2013b) A study on a water-inrush incident at Laohutai coal mine. Int J Rock Mech Min Sci 59:151–159

Li CY, Zuo JP, Shi Y, Wei CC, Duan YQ, Zhang Y, Yu H (2021a) Deformation and fracture at floor area and the correlation with main roof breakage in deep longwall mining. Nat Hazards 107(2):1731–1755

Li XL, Dong SN, Liu KD (2021b) Prevention and control of water inrushes from subseam karstic Ordovician limestone during coal mining above ultra-thin aquitards. Mine Water Environ 40(2):345–356

Lu YL, Wang LG (2015) Numerical simulation of mining-induced fracture evolution and water flow in coal seam floor above a confined aquifer. Comput Geotech 67:157–171

Ma D, Duan HY, Liu WT, Ma XT, Tao M (2020) Water–sediment two-phase flow inrush hazard in rock fractures of overburden strata during coal mining. Mine Water Environ 39(2):308–319

Ma K, Sun XY, Tang CA, Yuan FZ, Wang SJ, Chen T (2021) Floor water inrush analysis based on mechanical failure characters and microseismic monitoring. Tunn Undergr Space Technol 108:103698

Marroquin ID, Hart BS (2004) Seismic attribute-based characterization of coalbed methane reservoirs: an example from the Fruitland Formation, San Juan basin. New Mexico AAPG Bull 88(11):1603–1621

Meng XX, Liu WT, Zhao JY, Ding XY (2019) In situ investigation and numerical simulation of the failure depth of an inclined coal seam floor: a case study. Mine Water Environ 38(3):686–694

Mu WQ, Li LC, Yang TH, Yu GF, Han V (2019) Numerical investigation on grouting mechanism with slurry-rock coupling and shear displacement in single rough fracture. Bull Eng Geol Environ 78(8):6159–6177

Mu WQ, Wang DY, Li LC, Yang TH, Feng QB, Wang SX, Xiao FK (2021) Cement flow in interaction rock fractures and its corresponding new construction process in slope engineering. Constr Build Mater 303(11):124533

Niu HG, Wei JC, Yin HY, Xie DL, Zhang WJ (2020) An improved model to predict the water-inrush risk from an Ordovician limestone aquifer under coal seams: a case study of the Longgu coal mine in China. Carbonates Evaporites 35(3):73

Ren B, Mu WQ, Jiang BY, Yu GF, Li LC, Wei TS, Han YC, Xiao DC (2021) Grouting mechanism in water-bearing fractured rock based on two-phase flow. Geofluids 2021:5585288

Salimiana MH, Baghbanana A, Hashemolhosseini H, Dehghanipoodeh M, Norouzi S (2017) Effect of grouting on shear behavior of rock joint. Int J Rock Mech Min Sci 98:159–166

Shi LQ, Qu XY, Yu XG, Li Y, Pei FH, Qiu M, Gao WF (2020) Theory and practice on the division of the "water pressure-free zone" in a mining coal seam floor. Arab J Geosci 13(20):1079

Song WC, Liang ZZ (2021) Theoretical and numerical investigations on mining-induced fault activation and groundwater outburst of coal seam floor. Bull Eng Geol Environ 80(7):5757–5768

Song CG, Yao LH, Gao J, Hua CY, Ni QH (2021) Identification model of water inrush source based on statistical analysis in Fengyu minefield. Northwest China Arab J Geosci 14(6):518

Stromsvik H (2019) The significance of hydraulic jacking for grout consumption during high pressure pre-grouting in Norwegian tunnelling. Tunn Undergr Space Technol 90:357–368

Sun WB, Xue YC, Li TT, Liu WT (2019) Multi-field coupling of water inrush channel formation in a deep mine with a buried fault. Mine Water Environ 38(3):528–535

Wang JC, Li JB (2010) Physical model and theoretic criterion of the forecast of water inrush caused by collapse columns. J Univ Sci Tech Beijing 32(10):1243–1247 (**in Chinese**)

Wang JC, Yang SL (2009) Numerical simulation of mining effect on water flowing mechanism of collapse column activation. J Min Safe Eng 26(2):140–144 (**in Chinese**)

Wu JS, Cai JC, Zhao DY, Chen XX (2014) An analysis of mine water inrush based on fractal and non-Darcy seepage theory. Fractals-Complex Geom Patterns Scaling Nat Soc 22(3):1440008

Wu Q, Guo XM, Shen JJ, Xu S, Liu SQ, Zeng YF (2017) Risk assessment of water inrush from aquifers underlying the Gushuyuan coal mine. China Mine Water Environ 36(1):96–103

Wu Q, Mu WP, Xing Y, Qian C, Shen JJ, Wang Y, Zhao DK (2019) Source discrimination of mine water inrush using multiple methods: a case study from the Beiyangzhuang Mine. Northern China Bull Eng Geol Environ 78(1):469–482

Wu Q, Du ZL, Zhao YW, Xu H, Zhang XY (2021) Optimal location of water level sensors for monitoring mine water inrush based on the set covering model. Sci Rep 11(1):2621

Xu ZM, Sun YJ, Gao S, Chen HY, Yao MH, Li X (2021) Comprehensive exploration, safety evaluation and grouting of karst collapse columns in the Yangjian coalmine of the Shanxi province. China Carbonates Evaporites 36(1):16

Yang B, Yang TH, Jun Hu (2021) Numerical simulation of non-Darcy flow caused by cross-fracture water inrush, considering particle loss. Mine Water Environ 40(2):466–478

Yu HT, Zhu SY, Wang XH (2021) Research on groundwater seepage through fault zones in coal mines. Hydrogeol J 29(4):1647–1656

Yuan JQ, Chen WZ, Tan XJ, Yang DS, Zhang QY (2020) New method to evaluate antiwashout performance of grout for preventing water-inrush disasters. Int J Geomech 20(2):6019021

Zhang JC (2005) Investigations of water inrushes from aquifers under coal seams. Int J Rock Mech Min Sci 42(3):350–360

Zhang YJ (2021) Mechanism of water inrush of a deep mining floor based on coupled mining pressure and confined pressure. Mine Water Environ 40(2):366–377

Zhang SC, Guo WJ, Li YY, Sun WB, Yin DW (2017) Experimental simulation of fault water inrush channel evolution in a coal mine floor. Mine Water Environ 36(3):443–451

Zhang J, Chen LW, Li J, Chen YF, Ren XX, Shi XP (2021) Analysis of mining effects on the geochemical evolution of groundwater, Huaibei coalfield. China Environ Earth Sci 80(3):98

Zhao Y, Yang TH, Zhang PH, Xu HY, Wang SH (2020a) Inversion of seepage channels based on mining-induced microseismic data. Int J Rock Mech Min Sci 126:104180

Zhao Y, Wang CL, Bi J (2020b) Analysis of fractured rock permeability evolution under unloading conditions by the model of elastoplastic contact between rough surfaces. Rock Mech Rock Eng 12:5795–5808

Zhou JR, Yang TH, Zhang PH, Xu T, Wei J (2017) Formation process and mechanism of seepage channels around grout curtain from microseismic monitoring: a case study of Zhangmatun iron mine, China. Eng Geol 226:301–315

Zhou FD, Fredericks L, Luft J, Oraby M, Jeffries M, Keogh S (2020) A case study of mapping igneous sill distribution in coal measures using borehole and 3D seismic data. Int J Coal Geol 227:103531

Zuo JP, Peng SP, Li YJ, Chen ZH, Xie HP (2009) Investigation of karst collapse based on 3-D seismic technique and DDA method at Xieqiao coal mine. China Int J Coal Geol 78(4):276–287